Interpenetration of Interacting Polyelectrolytes

Devesh Srivastava and M. Muthukumar*

Polymer Science and Engineering Department and Materials Research Laboratory, University of Massachusetts, Amherst, Massachusetts 01003

Received August 2, 1993; Revised Manuscript Received December 2, 1993•

ABSTRACT: We have studied the structure of aggregates formed by oppositely charged polyelectrolytes of the same chain length N and charge density and the kinetics of the formation of these aggregates using a dynamic Monte Carlo algorithm. The model considers the evolution of chains through local motion of monomers and exhibits the complex behavior associated with the formation of such aggregates. The chains interpenetrate in two distinct steps—the chains first diffuse toward each other and then collapse abruptly to form smaller aggregates. This abrupt collapse is a consequence of cooperativity in the aggregation process. The chains collapse and are considerably smaller in the aggregate than in isolation; the conformational properties of each of the two chains of the same chain length and charge density in the aggregate are the same. The radii of gyration of the chains in the aggregate and of the aggregate scale as $N^{1/2}$. Aggregates formed by longer chains initially scale as N. These aggregates continue to reorganize and eventually scale as $N^{1/2}$. However, it is possible that for sufficiently long chains, as in real experimental situations, this process of reorganization is hindered by the formation of entanglements, etc. The aggregates would then form a nonequilibrium structure and would not scale as $N^{1/2}$.

I. Introduction

Specific interactions such as hydrogen-bonding and electrostatic interactions in macromolecules result in the formation of supramolecular structures in many applications such as ionomers and gels and exercise great influence on material behavior.[1-4] These structures form spontaneously and are characterized by a wide range of organization. The extent of organization is determined by molecular architecture and the strength of intermolecular interactions. Also, intermolecular interactions mediate molecular recognition in biological systems.

Electrostatic interactions are the strongest among molecular interactions and have been studied extensively experimentally. Although the behavior of uniformly charged polyelectrolytes in solution is well understood, a molecular understanding of the formation of aggregates by oppositely charged polyelectrolytes and of the kinetics of the formation of these aggregates is lacking at present. As a model system for interaction between chains we consider the interaction of two oppositely charged chains of the same chain length and charge density.

Baljon-Haakman and Witten[5] have recently studied the structure of two associating chains which are constrained to adhere to each other by *stickers*. Each chain, in this study, has two stickers located along its contour. A sticker can adhere to another sticker located on the same chain or to one located on the other chain. The stickers are free to exchange partners. This freedom to exchange partners leads to an increase in the number of possible conformations and amounts to an entropic attraction. This attractive interaction is offset by the repulsive interaction between two self-paired chains in a good solvent. Thus alteration of sticker placement can alter the balance between attraction and repulsion. The interaction between chains is found to be attractive if the ratio of the sticker distance to the chain length is 0.776 for symmetrically placed stickers and 0.826 for maximally asymmetrically placed stickers.

A simple physical model which exhibits the complex behavior associated with the formation of supramolecular structures has been used in this paper to study the aggregation of polyelectrolytes. In this model the polymer chains are represented as flexible linear molecules which evolve through local motion of monomers. Interactions between molecules have been modeled by ascribing to monomers a hard-core repulsive potential to represent excluded-volume interaction and by randomly locating charges of opposite sign along the chains; these charges interact through a screened Coulombic interaction. The paper has been organized as follows: the model and simulation technique have been detailed in section II; the results are presented in section III.

II. Model and Simulation Technique

In the simulation the polymer chains are represented as freely jointed chains—each chain consists of a series of N segments connected by freely rotating bonds of Kuhn length l. A randomly selected fraction f of monomers on chain 1 is assigned a charge +1, while a fraction f of those on chain 2 is assigned a charge −1. Each monomer is also ascribed a hard-core diameter $2a$ in order to account for excluded-volume interactions. The monomers interact through an excluded-volume interaction due to hard-core repulsion

$$V_1(r_{ij}) = \begin{cases} 0 & r_{ij} > a \\ \infty & r_{ij} \le a \end{cases}$$

and a screened Coulombic interaction[4] between charged monomers i and j given as

$$V_2(r_{ij}) = \frac{q_i q_j}{4\pi\epsilon}\frac{e^{-\kappa r_{ij}}}{r_{ij}}, \qquad r_{ij} = |r_i - r_j|$$

where r_{ij} is the separation between the ith and the jth monomer, q_i is the charge on the ith monomer, and κ is the inverse Debye–Huckel screening length given as

$$\kappa^2 = \frac{4\pi e^2}{\epsilon k T}\sum_i n_i^0 z_i^2$$

where n_i^0 is the number of z_i-valent ions in solution and e is the electronic charge; ϵ is the dielectric constant of the solvent. Also, k is the Boltzmann constant and T the absolute temperature. In these simulations the Kuhn step length l has been taken to be 2.5 Å and the hard-core diameter has been assumed to be $3^{1/2}l/2$. Also, the temperature has been taken to be 300 K, and the Debye–Huckel screening length, κ^{-1}, is assumed to be 50 Kuhn lengths.

• Abstract published in *Advance ACS Abstracts*, February 1, 1994.

0024-9297/94/2227-1461$04.50/0

The chains are allowed to evolve by a dynamic Monte Carlo algorithm described by Baumgartner.[6] This algorithm changes chain conformation by local motion of monomers. A monomer chosen at random is rotated through an angle ϕ about the axis defined by adjacent monomers to a new trial position. If the monomer chosen happens to lie at either end of the chain, it is moved through two randomly chosen angles θ and ϕ to a new trial position. If the monomer chosen does not overlap with other monomers at this new position and if it has a lower potential energy, the new conformation is accepted. If it has a higher potential energy, the new conformation is accepted if $e^{-\Delta E/kT}$ is less than a number chosen at random in the range [0,1]. The attempted move is counted even if the new trial conformation is not accepted. N such elementary moves represent one Monte Carlo time step.

The simulation is carried out in two stages. In stage 1, the chains do not interact with each other and configuration statistics, such as mean-squared radius of gyration R_g^2, for isolated chains are collected. In stage 2, two such chains are confined in a cube of side $5R_g$ with their centers of mass separated by a distance δ_0. Starting from this initial conformation, the chains are allowed to interact with each other. The conformations of interacting chains are changed by moving monomers, chosen at random, alternately on each chain. Configuration statistics for interacting chains are collected during this stage. Configuration statistics have been obtained by averaging over one thousand independent, *i.e.*, uncorrelated, conformations. These conformations were obtained by sampling chain conformations at intervals of N Monte Carlo time steps.

The initial distance of separation, δ_0, between the centers of mass of the two chains is chosen to be such that the chains do not overlap. This ensures that the starting conformation does not violate excluded-volume interaction between monomers on different chains. Simulations have been carried out for three different values of δ_0, *viz.*, R_g, $2R_g$, and $4R_g$. Differences in the values of δ_0 do not affect the structure of the aggregate. Weakly interacting chains move away in some cases and evolve independently of each other. However, when they do come together, they form aggregates like strongly interacting chains. In order to ensure that the chains do not move away, the chains are confined in a cube of side $5R_g$; this length is comparable to the size of the extended isolated chains and is much larger than the radius of gyration of the aggregates formed. The presence of the cube, therefore, does not affect the conformations of the aggregates. Moreover, the radius of gyration of the aggregates formed by unconfined chains is similar to that of aggregates formed by confined chains.

Simulations have been carried out to determine the influence of the number of segments N and the fraction f of charged monomers along the chain contour on the structure of the aggregate. Simulations have also been carried out to study the influence of changes in δ_0, the initial distance between the centers of mass of the chains, on the kinetics of formation of the aggregates.

III. Results and Discussion

A. Structure of the Aggregates. The conformations of the chains and the aggregates formed have been characterized by their mean-squared radii of gyration R_g^2

$$R_g^2 = \frac{l^2}{N^2}\sum_{i=1}^{N-1}\sum_{j=i+1}^{N}\langle[r_i - r_j]^2\rangle$$

where r_i is the position vector of the ith monomer and the angular brackets denote averaging over all possible chain conformations. The mean-squared radii of gyration of isolated and interacting chains, obtained by averaging over one thousand independent conformations for short chains ($N \leq 60$) and over ten thousand independent conformations for longer chains ($N > 60$), are plotted in Figure 1a–c for charge densities $f = 0.2$, 0.5, and 0.8 along the chain contour, respectively. The mean squared radii of gyration of the aggregates formed are also included in these figures.

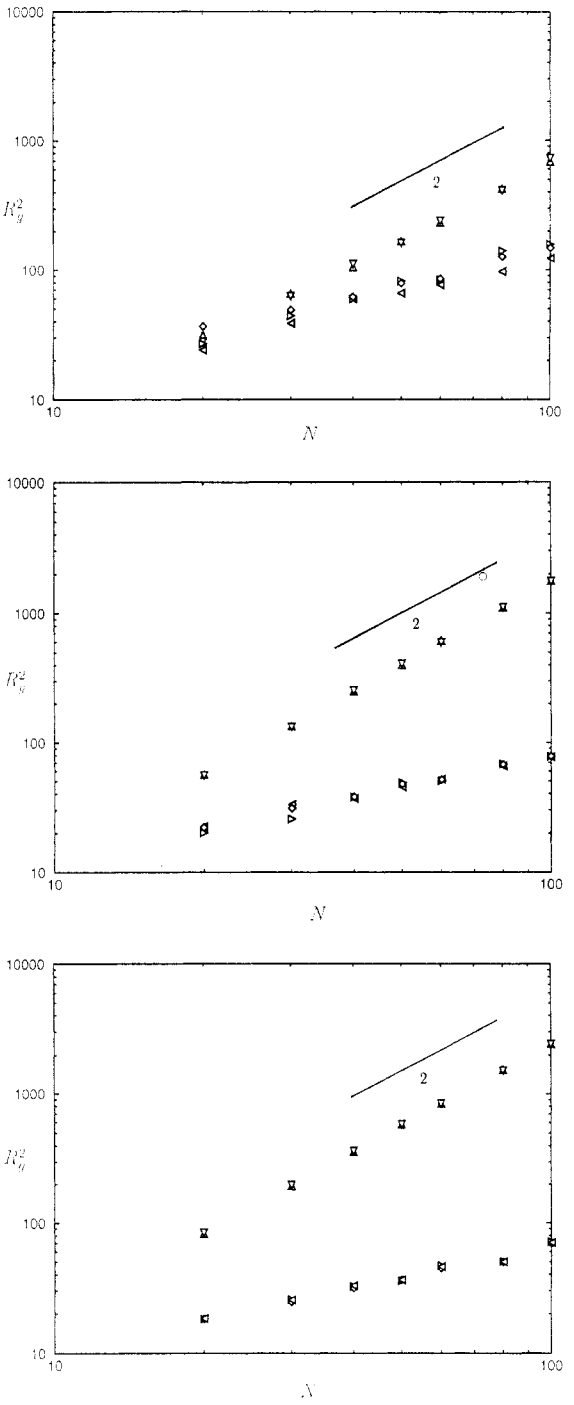

Figure 1. Mean-squared radii of gyration, R_g^2, of isolated and interacting chains and the aggregate *vs* the chain length N for $\kappa^{-1} = 50$ Kuhn lengths. (a) $f = 0.2$, (b) $f = 0.5$, and (c) $f = 0.8$. (△) Chain 1 in isolation. (▽) Chain 2 in isolation. (◁) Chain 1 in aggregate. (▷) Chain 2 in aggregate. (◇) The aggregate. A slope of 2.0 is included as a guide in these figures.

Simulations show that noninteracting chains exist in extended conformations characteristic of polyelectrolytes. The radius of gyration increases with the extent of ionization of the chains and with chain length because of electrostatic repulsion. The Debye–Huckel screening length is on the order of contour length of the chains. On the other hand, interacting chains form a smaller aggregate than the size of an individual isolated chain. The structure of this aggregate is determined by two competing factors—electrostatic attraction between chains which favors chain collapse and chain entropy which favors a swollen configuration. The aggregate is swollen if the electrostatic attraction is weak, i.e., when the chain is weakly ionized.

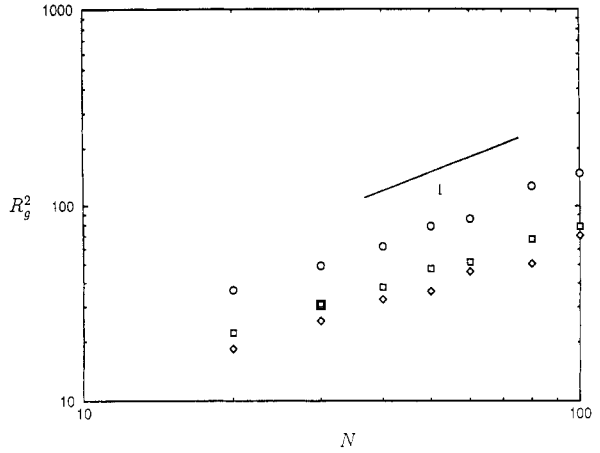

Figure 2. Mean-squared radius of gyration, R_g^2, of the aggregates *vs* the chain length N for $f = 0.2$ (○), 0.5 (□), and 0.8 (◇) and $\kappa^{-1} = 50$ Kuhn lengths. A slope of 1.0 is included as a guide in the figure.

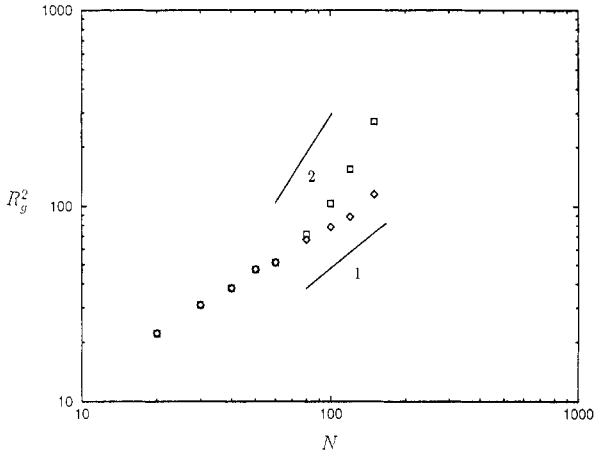

Figure 3. Mean-squared radius of gyration, R_g^2, of the aggregates *vs* the chain length N for $f = 0.5$ and $\kappa^{-1} = 50$ Kuhn lengths for averages obtained over one thousand conformations (□) and for averages obtained over ten thousand conformations (◇) for chain lengths 80, 100, 120, and 150. A slope of 1.0 and a slope of 2.0 are included as guides in the figure.

The radii of gyration of the aggregates formed by interacting chains for $f = 0.2, 0.5$, and 0.8 are plotted against the molecular weight in Figure 2. The radii of gyration of the chains in the aggregates and the radii of gyration of the aggregates scale as $N^{1/2}$; for chains with larger values of f the radius of gyration of the aggregate is found to be smaller. The effect of *annealing* on the structure of the aggregate has been studied by allowing the aggregate to evolve for a very long time. The radii of gyration of aggregates formed by longer chains, *viz.*, $N = 80, 100, 120$, and 150, for the case $f = 0.5$ obtained by averaging over one thousand conformations and over ten thousand conformations are shown in Figure 3. The radii of gyration in the first case scale with the molecular weight as N. However, when the aggregates are allowed to reorganize, as in the second case, the radii of gyration scale with the molecular weight as $N^{1/2}$. Thus, the radii of gyration of aggregates formed by longer chains initially scale as $R_g \sim N$; these aggregates continue to reorganize and the radii of gyration eventually scale as $R_g \sim N^{1/2}$. However, for sufficiently long chains this process of reorganization may be hindered by the formation of physical entanglements between chains. The aggregate would then form a nonequilibrium structure, and the radii of gyration of the aggregates would then scale with an exponent larger than $1/2$. The distribution of charges changes as aggregation occurs. As a result the Debye–Huckel screening length,

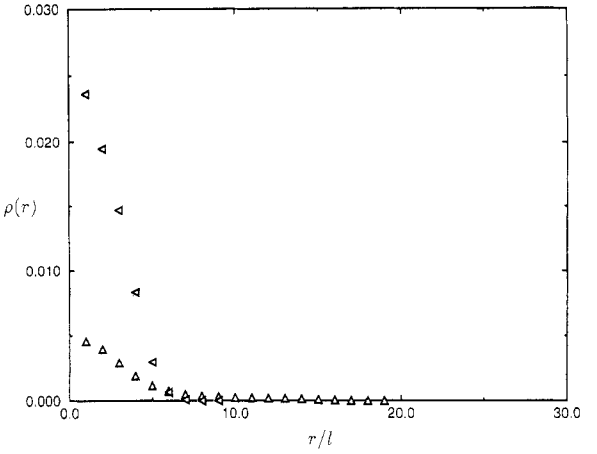

Figure 4. Radial density profile, $\rho(r)$, of (△) an isolated chain and (◁) an interacting chain in the aggregate *vs* the radial coordinate for $N = 50$, $f = 0.5$, and $\kappa^{-1} = 50$ Kuhn lengths. The radial coordinate has been normalized by the Kuhn length.

κ^{-1}, changes continuously during aggregation and a varying κ^{-1} should be used in the simulation. However, a single value of κ^{-1} has been used in the simulation described here. The simulations have been repeated with a 10 times smaller value of κ^{-1}, and the structure of the aggregates formed is found to be similar. Thus, changes in κ^{-1} during aggregation do not have a significant effect on the structure of the aggregates.

The radial monomer density distribution, obtained by averaging over one thousand different conformations of a chain, is plotted for a representative case, *viz.*, $N = 50$, in Figure 4 against the radial coordinate r. The radial coordinate has been normalized by the Kuhn length and has its origin at the center of mass. The fraction of charged monomers on the chains is 0.5. The isolated chain has a very broad distribution of density about the center of mass, and the density profile extends to a distance comparable to the contour length of the chain. However, in the aggregate the chain has a very sharply peaked distribution of density about the center of mass. Also, the profile extends to a smaller distance.

The conformations of isolated chains for $N = 50$ and $f = 0.5$ at the start of the second stage of the simulation when the chains begin to interact are shown in Figure 5a–c. It is evident from the x–y, y–z, and z–x projections shown that isolated chains adopt extended conformations typical of polyelectrolytes. The conformations of interacting chains after they have formed the aggregate have been depicted in Figure 5d–f. The chains in the aggregate interpenetrate and form a disordered network.

B. Kinetics of Aggregation. The kinetics of aggregation have been studied by following the distance between the centers of mass of the two chains and changes in the conformations of the chains during the simulation. The distance δ between the centers of mass of the chains is plotted against Monte Carlo time in Figure 6 for the representative case considered earlier, viz., $N = 50$, $f = 0.5$, and $\kappa^{-1} = 50$ Kuhn lengths for three different starting values of δ_0, viz., R_g, $2R_g$, and $4R_g$; the distance δ has been normalized by δ_0, the initial distance between the centers of mass of the chains when they begin to interact. The mean-squared radii of gyration of two interacting chains, each of chain length $N = 50$ and $f = 0.5$, have been plotted against Monte Carlo time in parts a and b of Figure 7, respectively.

Interacting chains diffuse toward each other until they first overlap. The conformation of interacting chains is unaffected by the presence of the other chain during this

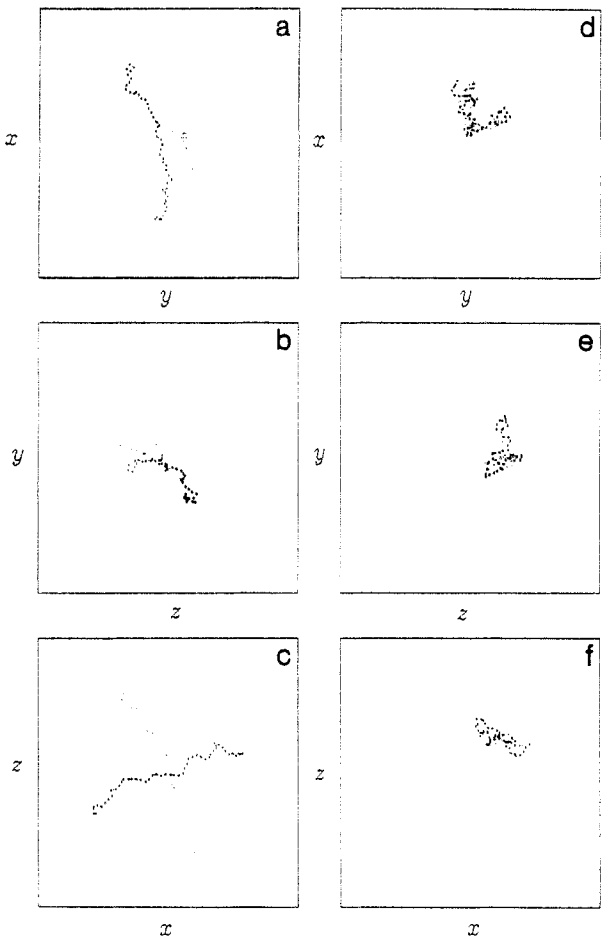

Figure 5. a–c correspond to x–y, y–z, and z–x projections of typical conformations of isolated chains. d–f correspond to x–y, y–z, and z–x projections of typical conformations of interacting chains for $N = 50$, $f = 0.5$, and $\kappa^{-1} = 50$ Kuhn lengths. The box corresponds to the cube used to confine the interacting chains.

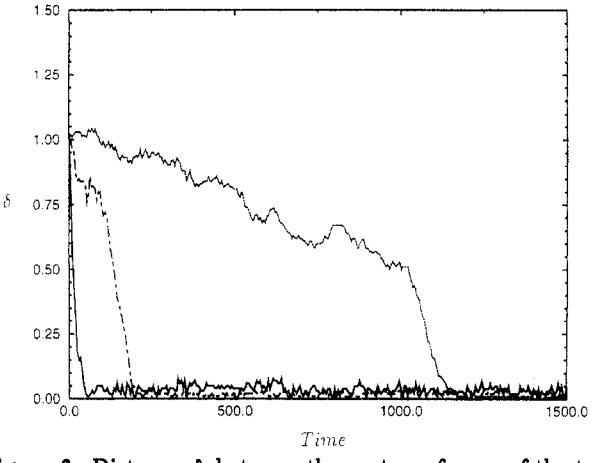

Figure 6. Distance, δ, between the centers of mass of the two interacting chains *vs* Monte Carlo time, in units of N, for $N = 50$, $f = 0.5$, and $\kappa^{-1} = 50$ Kuhn lengths. (—) $\delta_0 = R_g$, (– · –) $\delta_0 = 2R_g$, and (· · ·) $\delta = 4R_g$.

stage, and their radii of gyration are the same as that of isolated chains. The chains collapse into a smaller aggregate when they begin to interpenetrate, *i.e.*, when the distance between them is comparable to their radii. The aggregation is abrupt as is evident from the precipitate decrease in the distance δ between the chains and in their radii of gyration. The time at which the chains collapse depends on δ_0 and increases with δ_0 as shown in Figure 6. This abrupt collapse occurs because the chains are localized in space when the first physical *bond* is formed between

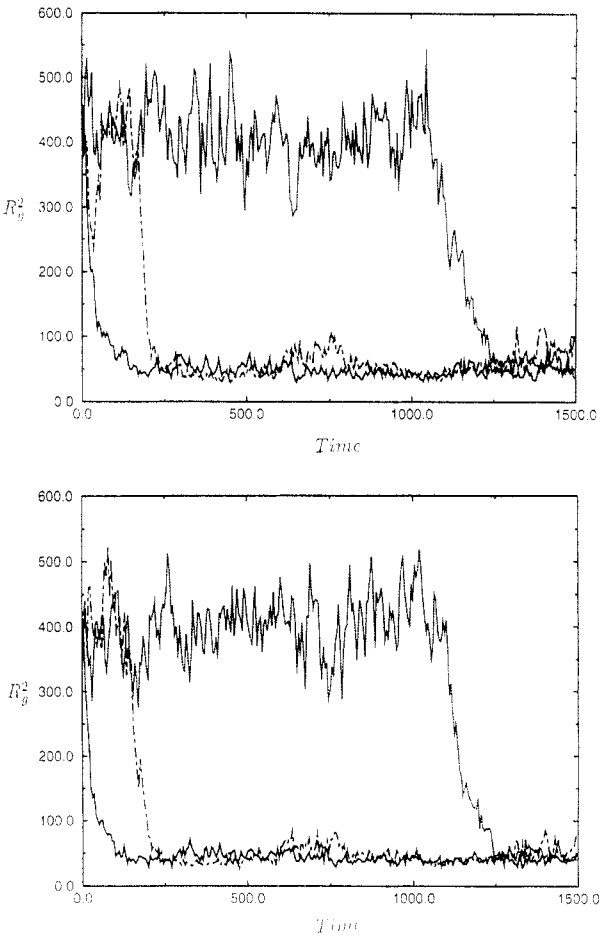

Figure 7. Instantaneous radius of gyration squared, $R_g^2(t)$, of interacting chains *vs* Monte Carlo time, in units of N, for $N = 50$, $f = 0.5$, and $\kappa^{-1} = 50$ Kuhn lengths: (a) chain 1; (b) chain 2. (—) $\delta_0 = R_g$, (– · –) $\delta_0 = 2R_g$, and (· · ·) $\delta = 4R_g$.

them. Localization results in a loss of translational freedom and hence of chain entropy. The loss of translational entropy leads to a much lower entropic barrier for the formation of subsequent bonds; as a result of this the subsequent bonds are formed extremely rapidly and the chains collapse into a smaller aggregate. Therefore, the aggregate is formed in two steps—the chains first diffuse toward each other and then collapse abruptly into a smaller aggregate. As a result, the rate at which aggregates are formed is limited by the rate at which the chains diffuse toward each other. Also, the abrupt collapse into a smaller aggregate is evidence of cooperativity in the formation of the aggregate. It is to be noted from Figure 7a,b that the fluctuations in the mean-squared radii of gyration of the chains are in registry; this suggests the occurrence of cooperative behavior between the two chains even before the aggregate is formed. Also, the distance between the two chains changes continually about a very small value. This suggests that the chains interpenetrate and continue to rearrange themselves in the aggregate.

The time-dependent mean-squared displacements, $R^2(t)$, of the centers of mass of the two chains were followed during the simulation, where

$$R^2(t) \equiv \langle [R_{CM}(t) - R_{CM}(0)]^2 \rangle$$

with $R_{CM}(t)$ being the position vector of the center of mass of a chain. Figure 8 contains the double-logarithmic plot of $R^2(t)$ of one of the chains in isolation and in the aggregate *vs* Monte Carlo time for the representative case, *viz.*, $N = 50$, $f = 0.5$, and $\kappa^{-1} = 50$ Kuhn lengths. It is evident from

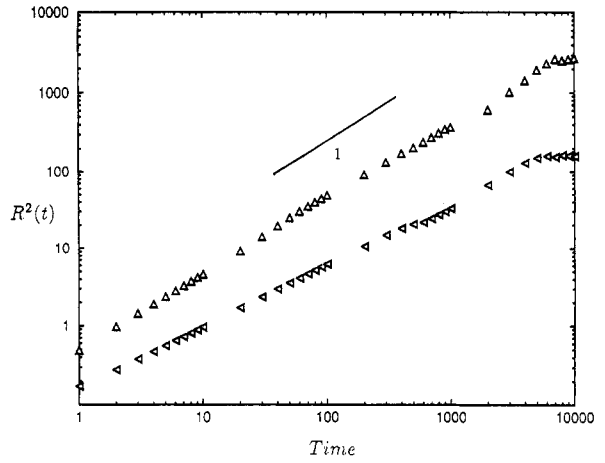

Figure 8. Mean-squared displacement, $R^2(t)$, of the center of mass of isolated and interacting chains *vs* Monte Carlo time, in units of N, for $N = 50$, $f = 0.5$, and $\kappa^{-1} = 50$ Kuhn lengths: (△) Chain in isolation; (◁) chain in the aggregate. A slope of 1.0 is included as a guide in the figure.

this figure that the motion of the chains in isolation can be described by classical diffusion, *viz.*, $\langle R^2 \rangle \sim t$. However, the mean-squared displacement of the chain in the aggregate is much smaller than that of the isolated chain. The smaller displacements and slope seen in the double-logarithmic plot for an interacting chain indicate that the chain is a part of a physical network. During the Monte Carlo time studied in the present simulation $\langle R^2 \rangle$ of an interacting chain in the aggregate is found to be proportional to t^α where the effective exponent α is about 0.8 and is expected to follow the diffusion law, $\alpha = 1$, at later times.

IV. Conclusions

Isolated chains adopt extended conformations because of repulsion between similar charges along the chain contour. However, in the presence of an oppositely charged chain of the same chain length and charge density the attraction between dissimilar charges on the chains results in the formation of smaller aggregates; the radii of gyration of these aggregates scale with the chain length as $N^{1/2}$. The chains in the aggregate form a scrambled physical network; this network reorganizes continually.

Aggregation occurs in two steps—the chains first diffuse toward each other until they overlap; overlapping chains then self-assemble into smaller aggregates. Self-assembly exhibits cooperative behavior. Isolated chains undergo classical diffusion; interacting chains, on the other hand, are a part of a physical network, and the centers of mass of the chains exhibit slower dynamics.

It would be of interest to study the influence of changes in variables such as temperature and the Debye–Huckel screening length on the structure of the aggregates and the kinetics of their formation. Also, a study of the influence of asymmetry in chain length and charge density on chain conformation may be of interest. Therefore, a study of more realistic models of interaction between polymer chains may lead to greater insight into the formation of structures such as coacervates and into self-assembly of complex molecules.

Acknowledgment is made to the Center for UMass—Industry Research in Polymers, the Materials Research Laboratory at the University of Massachusetts, and the NSF for Grant DMR 9008192. D.S. thanks Friedel von Goeler for help with the figures and J. J. Rajasekaran for useful discussions.

References and Notes

(1) Tsuchida, E.; Abe, K. *Adv. Polym. Sci.* **1982**, *45*, 1.
(2) Bekturov, E. A.; Kudaibergenov, S. E.; Rafikov, S. R. *J. Macromol. Sci., Rev. Macromol. Chem. Phys.* **1990**, *C30*, 233.
(3) Peiffer, D. G.; Lundberg, R. D. *Polymer* **1985**, *26*, 1058.
(4) Tanford, C. A. *Physical chemistry of macromolecules*; Wiley: New York, 1961.
(5) Baljon-Haakman, A. R. C.; Witten, T. A. *Macromolecules* **1992**, *25*, 2969.
(6) Baumgartner, A. In *Applications of the Monte Carlo Method in Statistical Physics*; Binder, K., Ed.; Springer: New York, 1984.